

Daily Research Report

Jeffrey Severino
University of Toledo
Toledo, OH 43606
email: jseveri@rockets.utoledo.edu

June 23, 2022

1 Current Research Direction

2 Research Performed

2.1 Results

Figure 1 shows the manufactured solution for the mean flow profile. The tangent summation method (TSM) was used to generate the axial mach number and for the speed of sound. The tangential mach number was then numerically approximated by using the composite trapezoidal rule. The manufactured mean flow profile is unique in that it has been generated solely for the verification of swirl and does not have physical significance. The “kinks” in the solution will allow there to be a significant magnitude for the derivatives of these solution.

The TSM was also used to generate the manufactured solutions for the perturbation variables in Figures 2-5. The boundary condition values of the MS for \bar{v}_r , dP/dr must reflect the actual boundary conditions in SWIRL. This is set by using a fairing function. Note that the hard wall condition requires \bar{v}_r to be zero which is shown in Figure 2. While the boundaries for the pressure perturbation may not be known, the boundary condition is set with the derivative of the pressure perturbation, which may or may not be zero depending if there is liner for the test case. This is why these functions no longer resemble tangent function, but in essence still are.

The results from the numerical integration is presented in Figure 6. Although the slope of the line appears linear, the TSM was still used to generate the MS for the speed of sound. To demonstrate the effect of using denser grids, the difference between the expected speed of sound to the actual speed of sound is shown in Figure 8 as a function of radius (needs label). Note that the error does not reach machine precision for the first grid and approaches zero as more grid points are used.

As the error decreases, it will decrease at a known rate depending on the numerical integration scheme used. Since the composite trapezoidal rule has an order of accuracy of 2, it is expected that the approximated order of accuracy will approach two as the error approaches zero. This behavior is shown in Figure 14 where the approximated line is the $L2_{norm}$ of the speed of sound error and the second order slope is an exponential function with a slope of 2 on a log-log plot. Although these data sets appear to be parallel, the slope is directly calculated to determine the value of this slope as the grid density increases. The slope (or the asymptotic rate of convergence)approached two for numerical integration as the grid spacing decreases (See Figure 15) .

For the LEE, a second and fourth order central differencing scheme is used for the approximated radial derivatives and then compared to the source terms generated for the MMS in Figure 9. (Discuss Error here...skeptical on the plot...13)

The $L2_{norm}$ and the asymptotic rate of convergence is shown for the two differencing schemes in 15 and 16. (How should is dicuss this?)

...

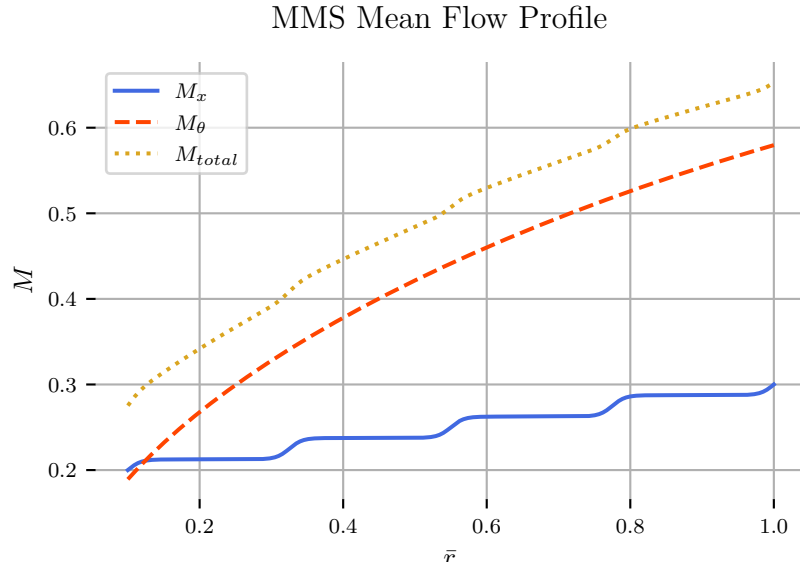


Figure 1: The manufactured mean flow test case using a summation of Tangents for A and M_x

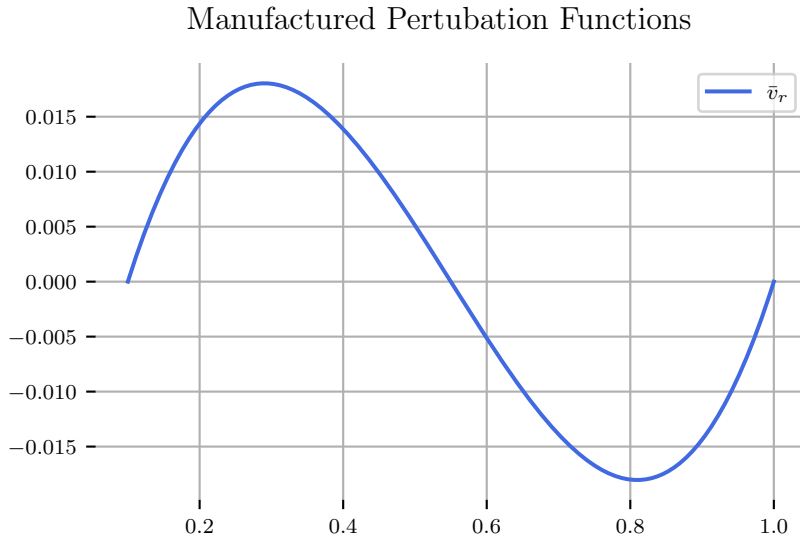


Figure 2: The manufactured perturbation functions \bar{v}_r

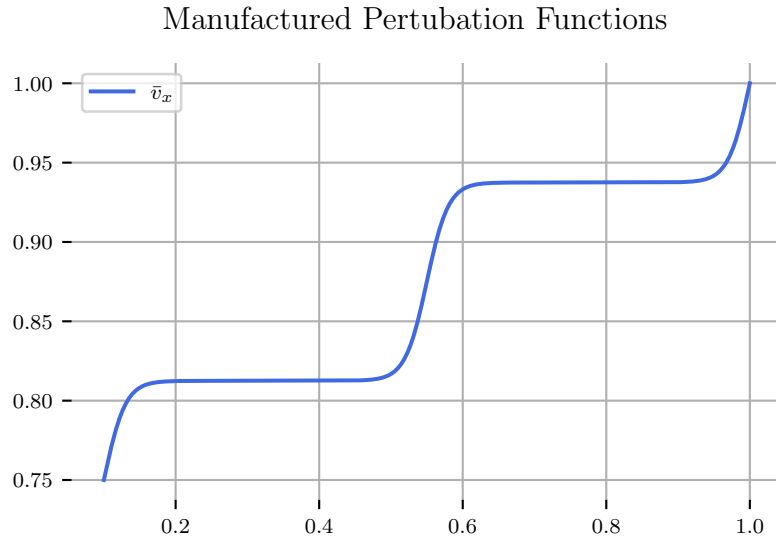


Figure 3: The manufactured perturbation functions \bar{v}_x

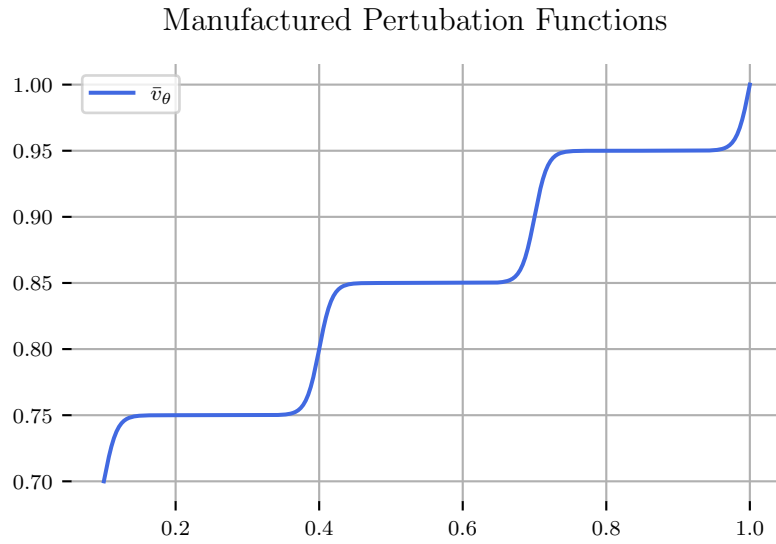


Figure 4: The manufactured perturbation functions \bar{v}_θ

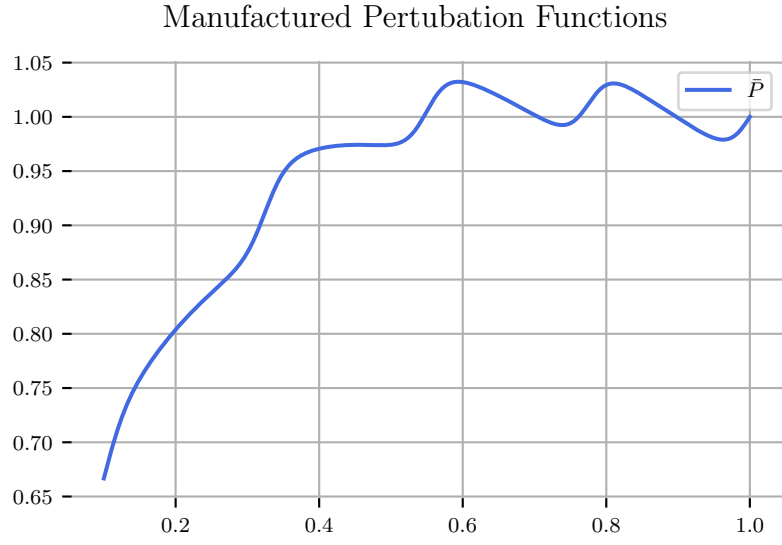


Figure 5: The manufactured perturbation functions , \bar{P}

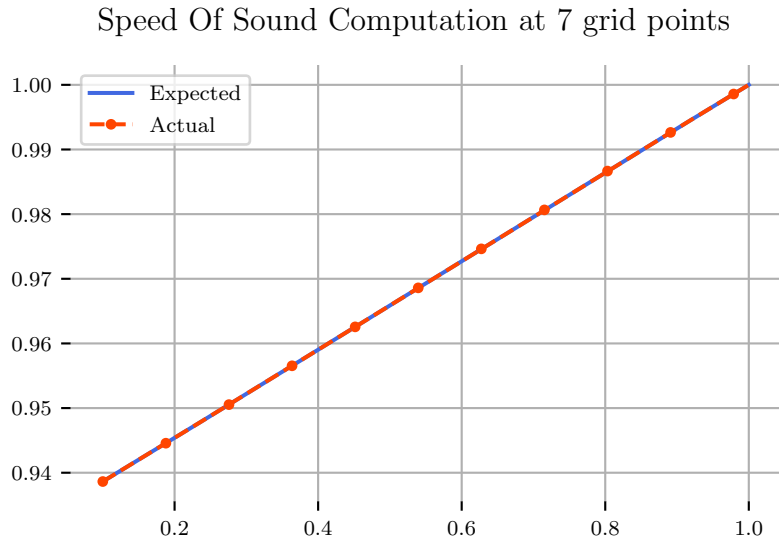


Figure 6: A comparison of the speed of sound, expected vs actual at the lowest grid to show similarities in solution

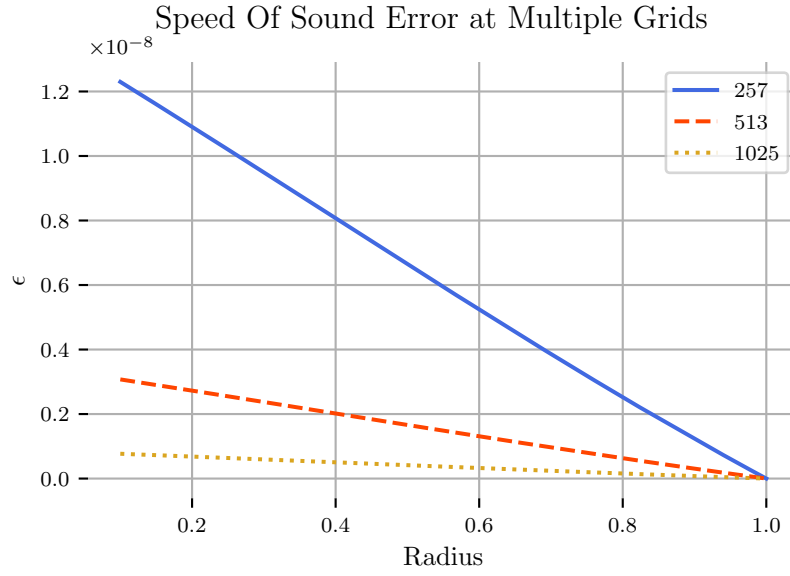


Figure 7: A comparison of the speed of sound error at three grid

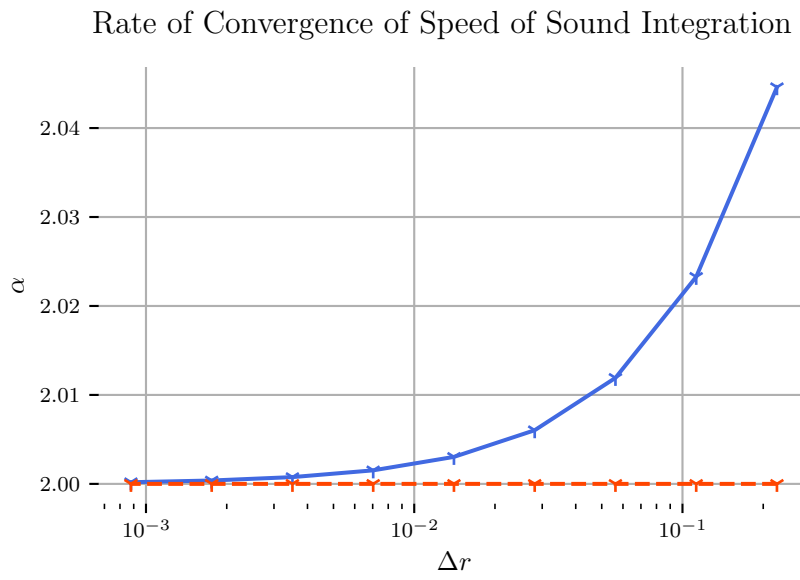


Figure 8: A comparison of the speed of sound error at three grid

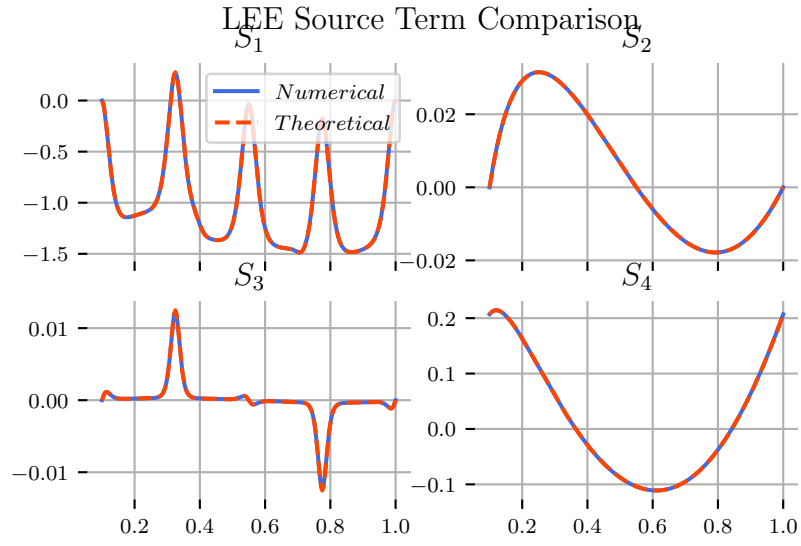


Figure 9: LEE Source Terms

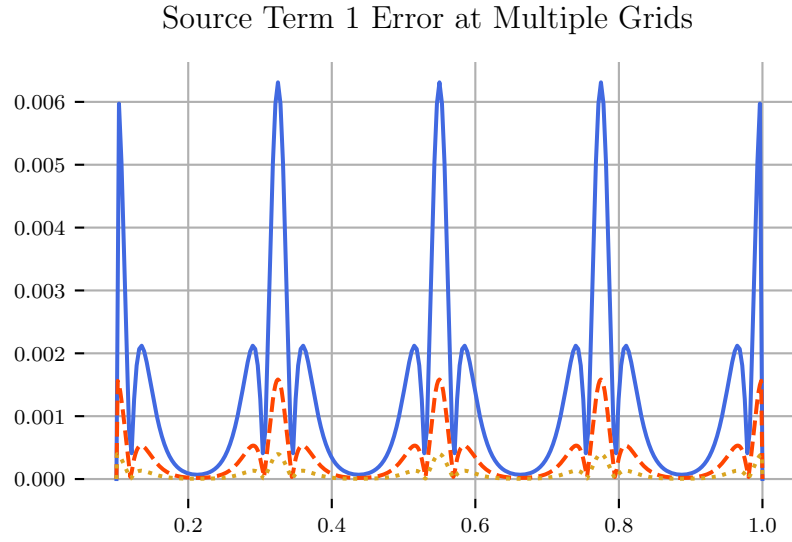


Figure 10: LEE Source Term Error

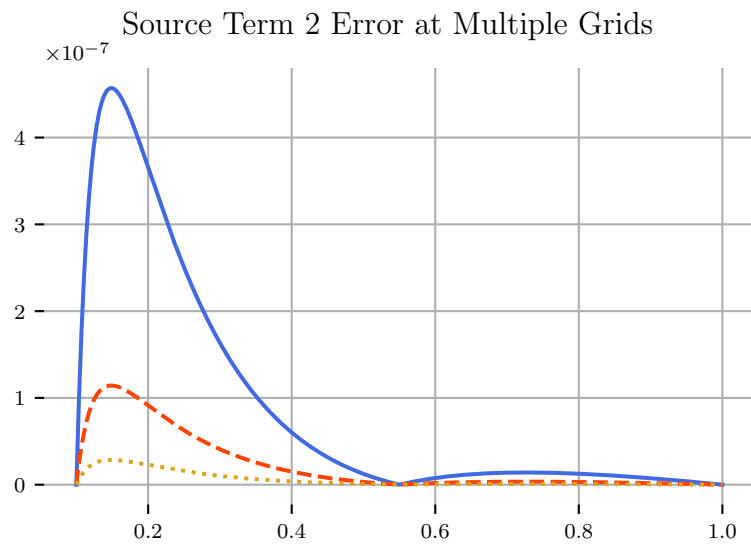


Figure 11: LEE Source Term Error

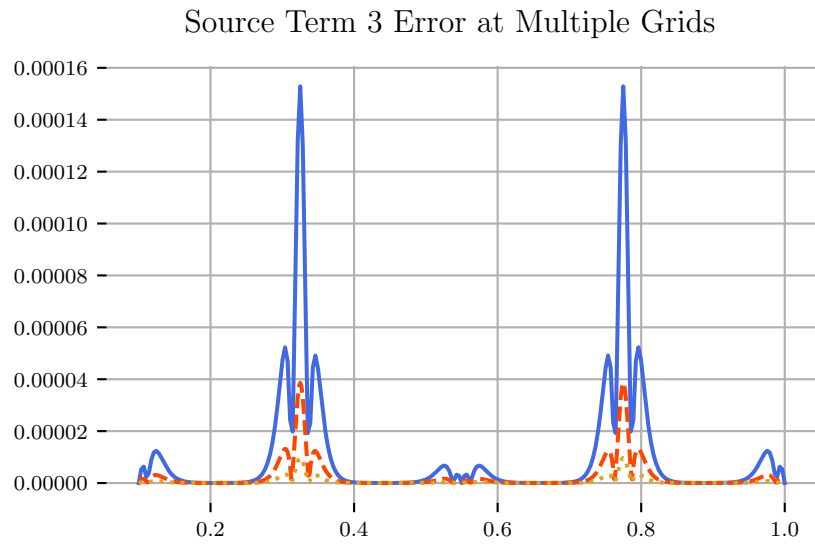


Figure 12: LEE Source Term Error

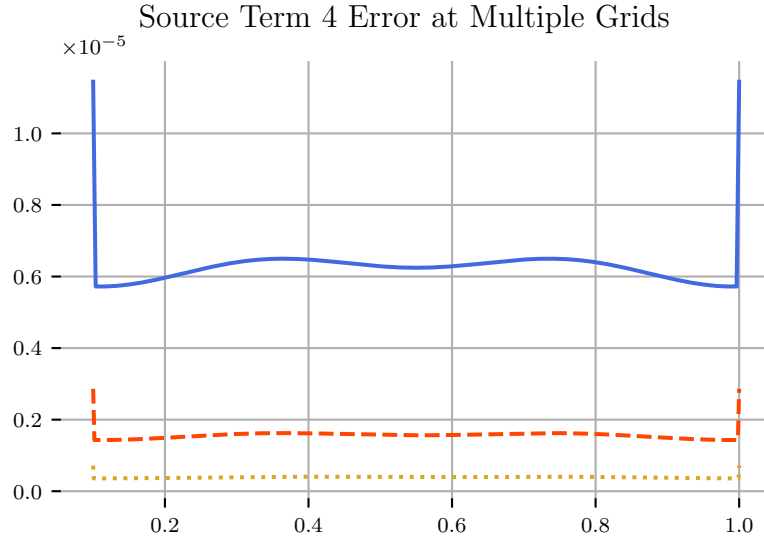


Figure 13: LEE Source Term Error

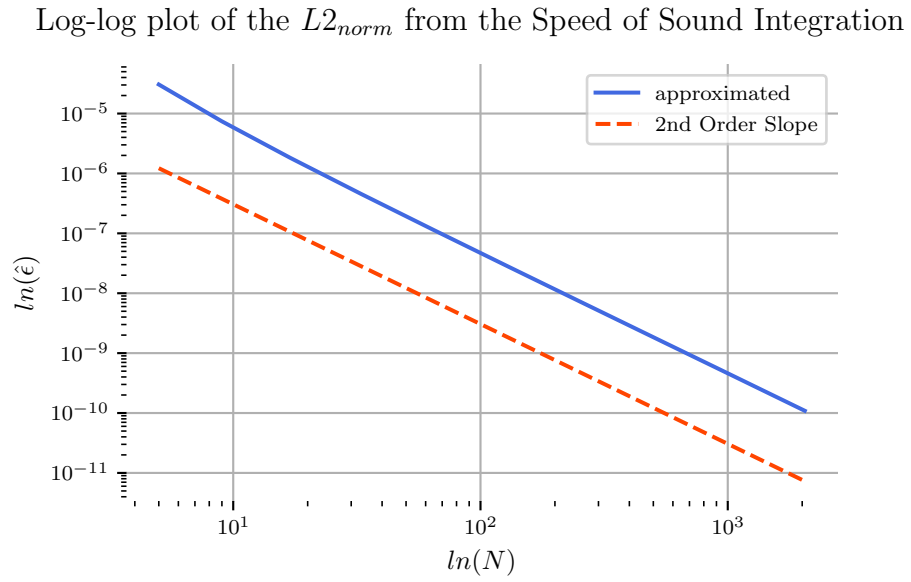


Figure 14: L2 Norm comparison for the speed of sound integration for the compound trapezoidal rule

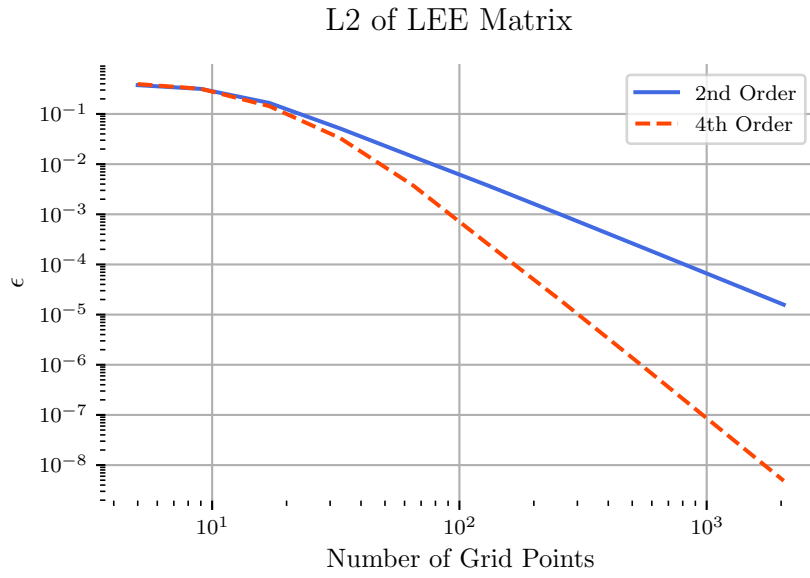


Figure 15: ROC for the speed of sound integration for the compound trapezoidal rule

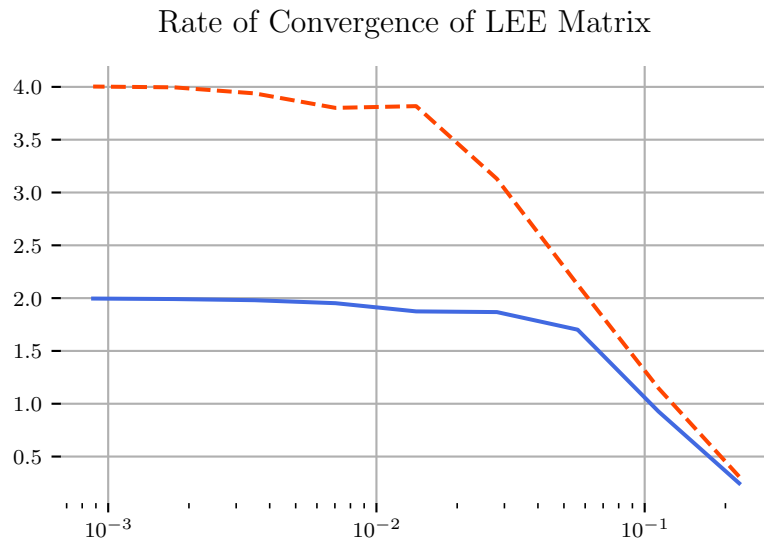


Figure 16: ROC for the LEE using second and fourth order central differencing for the radial derivative

3 Issues and Concerns

- Need to change title in speed of sound comparison. - Discuss the ROC for the second and fourth order schemes. - I would prefer to discuss the results separately.

4 Planned Research

Report MES.